

## Supporting Information

### Motif for B/O-sites modulation in LaFeO<sub>3</sub> towards boosted oxygen evolution

Wenli Kang<sup>a</sup>, Zhishan Li<sup>a\*</sup>, Jinsong Wang<sup>b</sup>, Shaopeng Wu<sup>a</sup>, Yiguang Gai<sup>a</sup>, Guanghao Wang<sup>a</sup>, Zhouhang Li<sup>a</sup>, Xing Zhu<sup>a</sup>, Tao Zhu<sup>a</sup>, Hua Wang<sup>a</sup>, Kongzhai Li<sup>a\*</sup>, Chundong Wang<sup>c</sup>

<sup>a</sup> Faculty of Metallurgical and Energy Engineering, Kunming University of Science and Technology, Kunming 650093, PR China

<sup>b</sup> Faculty of Materials Science and Engineering, Kunming University of Science and Technology, Kunming 650093, PR China

<sup>c</sup> School of Intergrated Circuits, Wuhan National Laboratory for Optoelectronics, Huazhong University of Science and Technology, Wuhan 430074, PR China

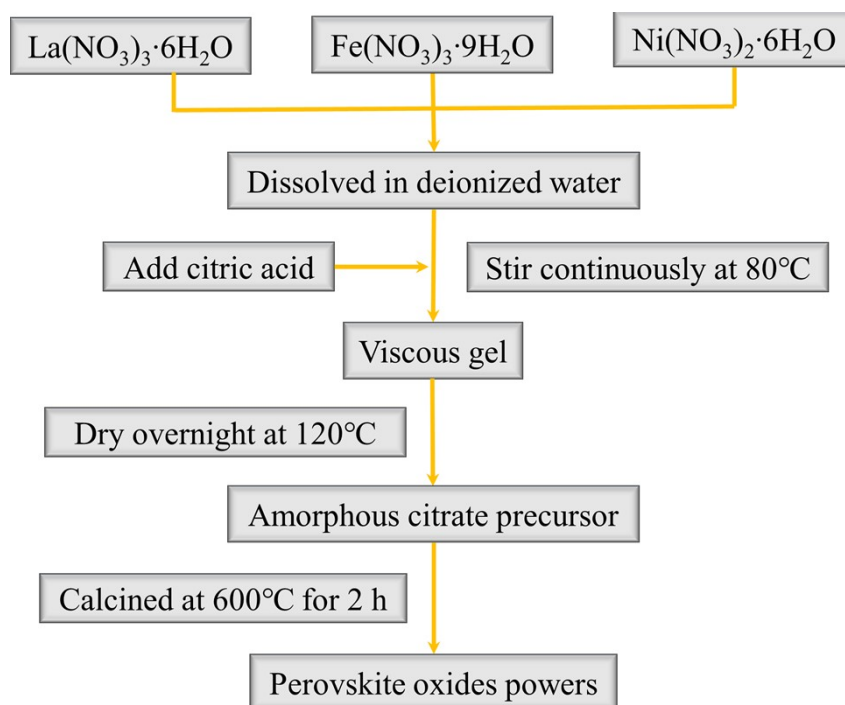


Fig. S1. Detail experiment procedures for fabrication of LaFe<sub>1-x</sub>Ni<sub>x</sub>O<sub>3-δ</sub> electrocatalysts with different Ni-concentration synthesized at 600°C.

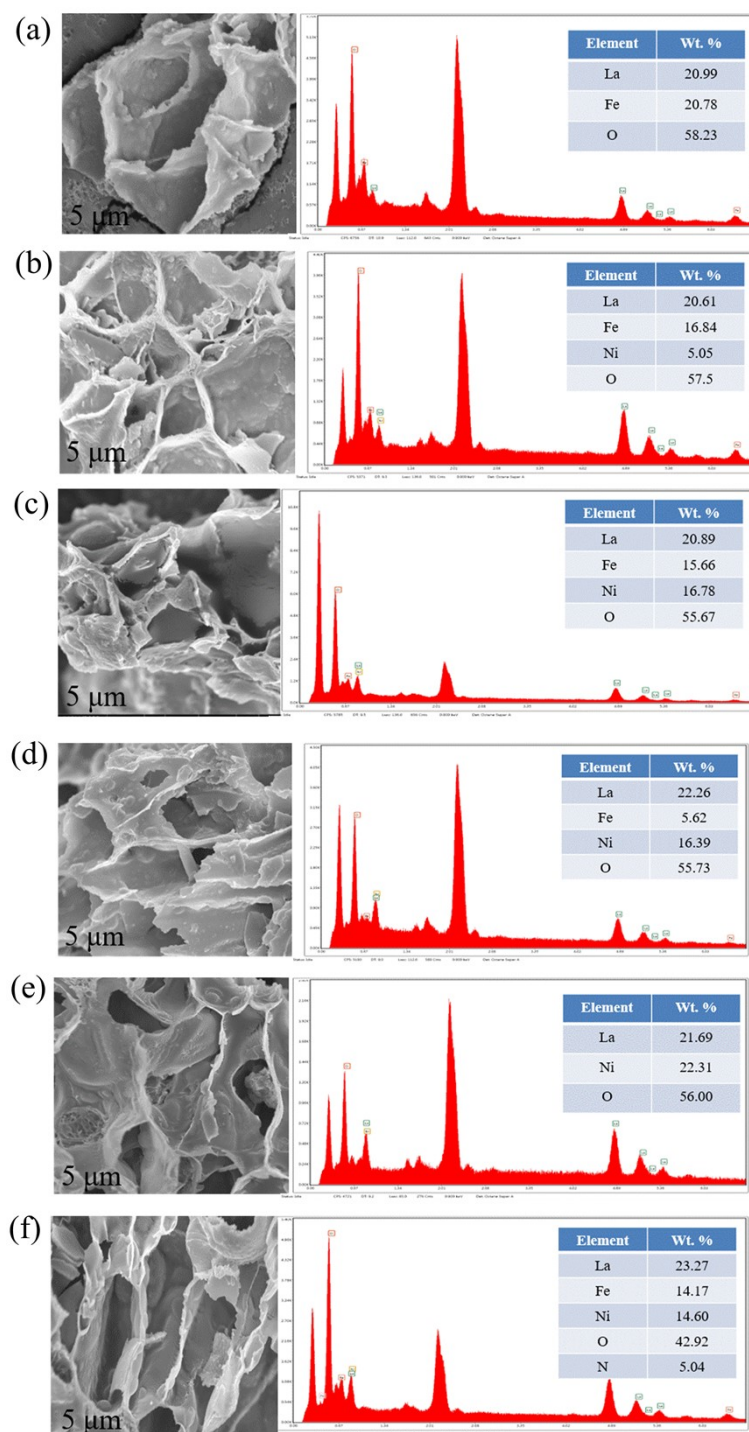


Fig. S2. SEM and EDS of (a)  $\text{LaFeO}_{3-\delta}$ , (b)  $\text{LaFe}_{0.75}\text{Ni}_{0.25}\text{O}_{3-\delta}$ , (c)  $\text{LaFe}_{0.5}\text{Ni}_{0.5}\text{O}_{3-\delta}$ , (d)  $\text{LaFe}_{0.25}\text{Ni}_{0.75}\text{O}_{3-\delta}$ , (e)  $\text{LaNiO}_{3-\delta}$ , and (f)  $\text{LaFe}_{0.5}\text{Ni}_{0.5}\text{O}_{3-\delta}/\text{N}$  catalysts (Inset is the corresponding element atoms percentage).

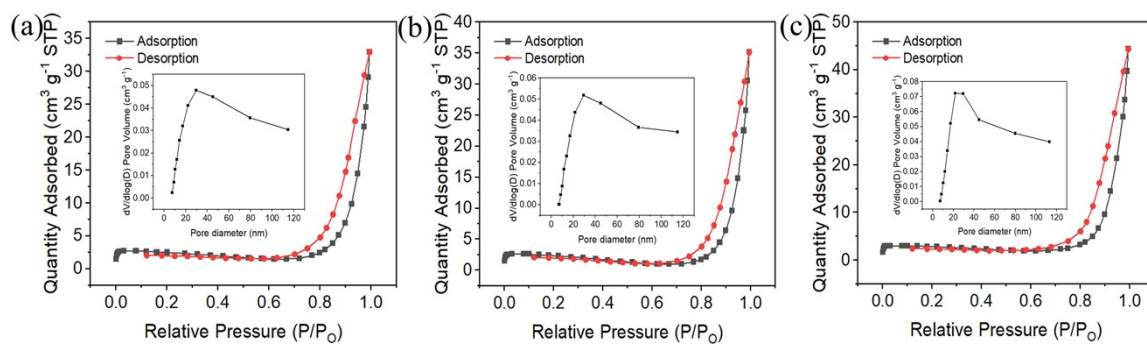


Fig. S3. Nitrogen adsorption-desorption hysteresis curve of (a)  $\text{LaFeO}_{3-\delta}$ , (b)  $\text{LaFe}_{0.5}\text{Ni}_{0.5}\text{O}_{3-\delta}$ , (c)  $\text{LaFe}_{0.5}\text{Ni}_{0.5}\text{O}_{3-\delta}/\text{N}$  catalysts (inset is the corresponding BJH pore size distribution curves).

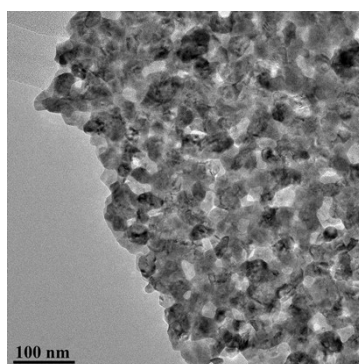


Fig. S4. TEM image of  $\text{LaFe}_{0.5}\text{Ni}_{0.5}\text{O}_{3-\delta}$ .

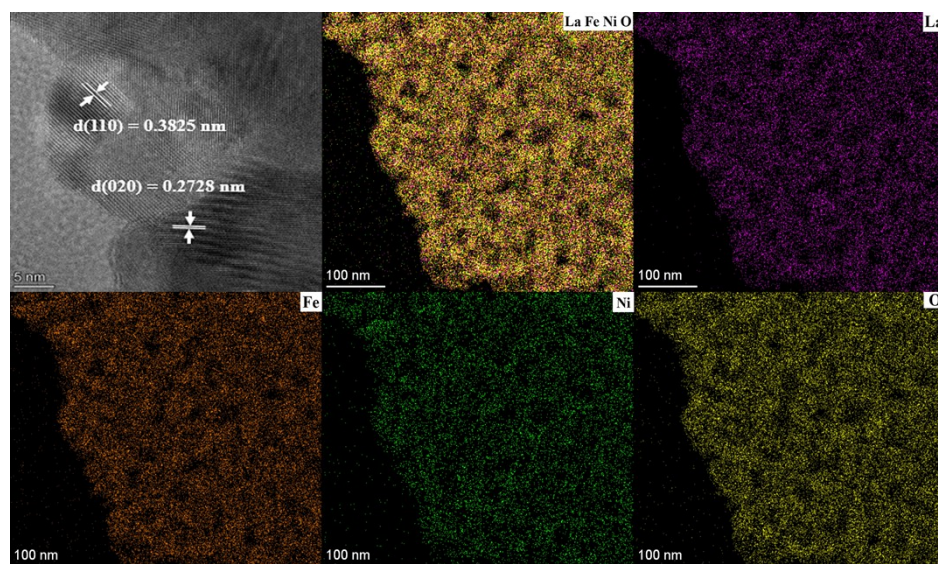


Fig. S5. HRTEM image of  $\text{LaFe}_{0.5}\text{Ni}_{0.5}\text{O}_{3-\delta}$  and the corresponding elemental mapping images of La, Fe, Ni, O.

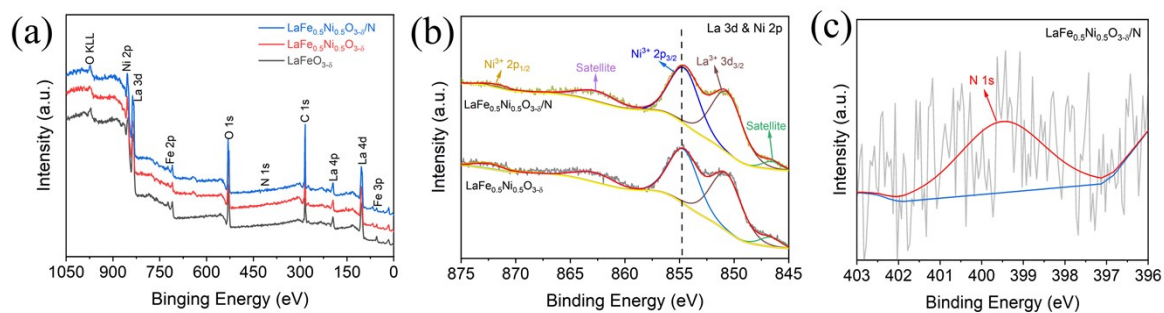


Fig. S6. (a) X-ray photoemission survey spectra of  $\text{LaFeO}_{3-\delta}$ ,  $\text{LaFe}_{0.5}\text{Ni}_{0.5}\text{O}_{3-\delta}$  and  $\text{LaFe}_{0.5}\text{Ni}_{0.5}\text{O}_{3-\delta}/\text{N}$ . (b-c) X-ray photoemission spectra of  $\text{LaFe}_{0.5}\text{Ni}_{0.5}\text{O}_{3-\delta}$  and  $\text{LaFe}_{0.5}\text{Ni}_{0.5}\text{O}_{3-\delta}/\text{N}$ . Each panel are corresponding binding energy range to (b) La3d & Ni2p and (c) N1s.

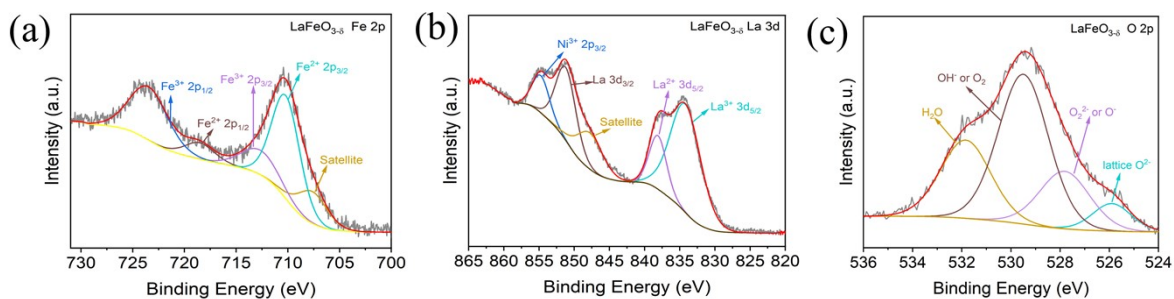


Fig. S7. (a-c) X-ray photoemission spectra of  $\text{LaFeO}_{3-\delta}$ . Each panel are corresponding binding energy range to (a) Fe 2p, (b) La 3d and (c) O 2p.

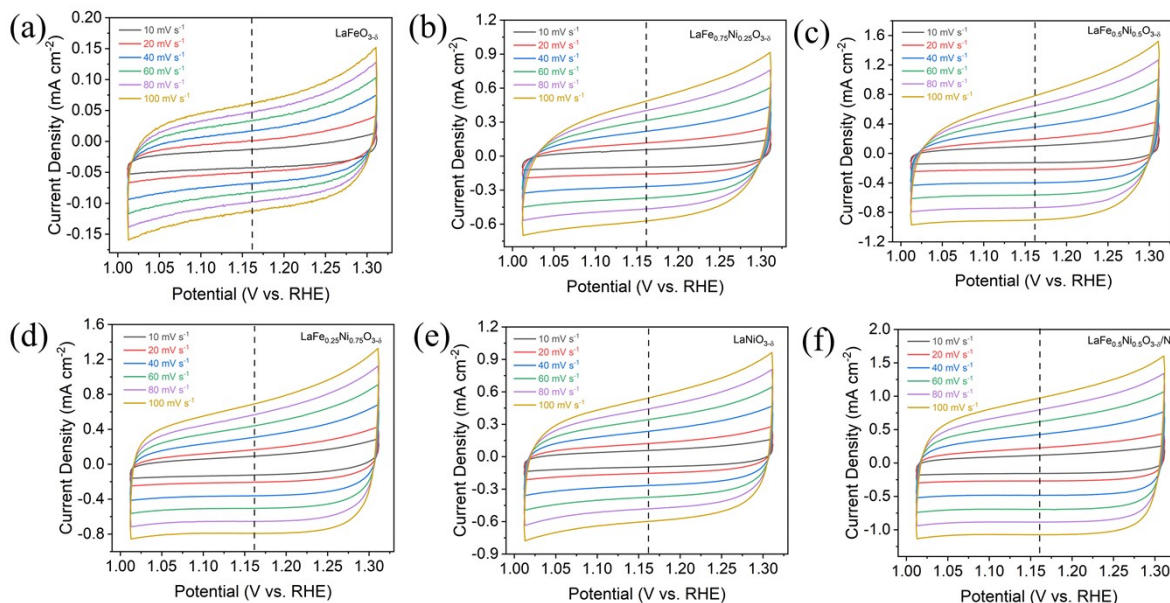


Fig. S8. CV measurements at different scan rates in a non-faradic current region with the scan interval of 100 mV s<sup>-1</sup> for (a) LaFeO<sub>3-δ</sub>, (b) LaFe<sub>0.75</sub>Ni<sub>0.25</sub>O<sub>3-δ</sub>, (c) LaFe<sub>0.5</sub>Ni<sub>0.5</sub>O<sub>3-δ</sub>, (d) LaFe<sub>0.25</sub>Ni<sub>0.75</sub>O<sub>3-δ</sub>, (e) LaNiO<sub>3-δ</sub>, and (f) LaFe<sub>0.5</sub>Ni<sub>0.5</sub>O<sub>3-δ</sub>/N catalysts.

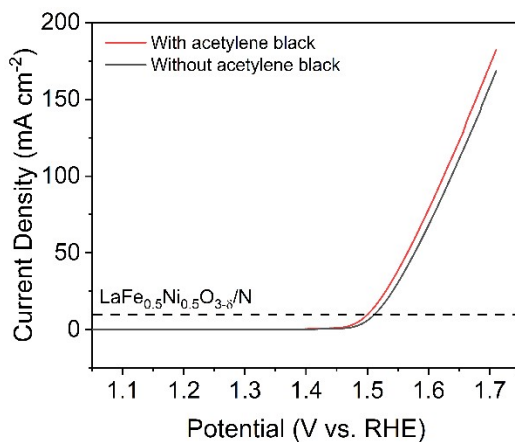


Fig. S9 Comparison of LSV polarization curves of sample LaFe<sub>0.5</sub>Ni<sub>0.5</sub>O<sub>3-δ</sub>/N with and without acetylene black.

Table S1. Atoms ratios of the  $\text{LaFe}_{1-x}\text{Ni}_x\text{O}_{3-\delta}$  ( $x = 0, 0.25, 0.5, 0.75, 1$ ) and  $\text{LaFe}_{0.5}\text{Ni}_{0.5}\text{O}_{3-\delta}/\text{N}$  derived from EDS analysis.

Element	La /wt%	Fe /wt%	Ni /wt%	O /wt%	N /wt%
<b>LaFeO<sub>3-δ</sub></b>	20.99%	20.78%	\	58.23%	\
<b>LaFe<sub>0.75</sub>Ni<sub>0.25</sub>O<sub>3-δ</sub></b>	20.61%	16.84%	5.05%	57.50%	\
<b>LaFe<sub>0.5</sub>Ni<sub>0.5</sub>O<sub>3-δ</sub></b>	20.89%	15.66%	16.78%	55.67%	\
<b>LaFe<sub>0.25</sub>Ni<sub>0.75</sub>O<sub>3-δ</sub></b>	22.26%	5.62%	16.39%	55.73%	\
<b>LaNiO<sub>3-δ</sub></b>	21.69%	\	22.31%	56.00%	\
<b>LaFe<sub>0.5</sub>Ni<sub>0.5</sub>O<sub>3-δ</sub>/N</b>	23.27%	14.17%	14.60%	42.92%	5.04%

Table S2. The details of the standard crystal planes of the reported materials.

Materials	Crystal planes (h k l)	d (Å)	2θ (°)	Intensity (a.u.)
LaFe <sub>0.5</sub> Ni <sub>0.5</sub> O <sub>3</sub>	020	2.7356	32.710	31.7
	110	3.8852	22.871	18.5

Table S3. Atoms ratios of the  $\text{LaFeO}_{3-\delta}$ ,  $\text{LaFe}_{0.5}\text{Ni}_{0.5}\text{O}_{3-\delta}$ , and  $\text{LaFe}_{0.5}\text{Ni}_{0.5}\text{O}_{3-\delta}/\text{N}$  derived from XPS analysis.

Element (Atomic %)	Electrocatalysts		
	$\text{LaFeO}_{3-\delta}$	$\text{LaFe}_{0.5}\text{Ni}_{0.5}\text{O}_{3-\delta}$	$\text{LaFe}_{0.5}\text{Ni}_{0.5}\text{O}_{3-\delta}/\text{N}$
<b>La 3d</b>	9.15	9.54	8.93
<b>Fe 2p</b>	8.06	5.84	6.11
<b>Ni 2p</b>	\	6.01	6.65
<b>O 1s</b>	37.33	35.04	30.43
<b>N 2s</b>	\	\	2.35
<b>C 1s</b>	45.46	43.57	45.53

Table S4. O 1s XPS deconvolution results of the  $\text{LaFeO}_{3-\delta}$ ,  $\text{LaFe}_{0.5}\text{Ni}_{0.5}\text{O}_{3-\delta}$ , and  $\text{LaFe}_{0.5}\text{Ni}_{0.5}\text{O}_{3-\delta}/\text{N}$ .

Element	$\text{H}_2\text{O}$	$\text{OH}^-$ or $\text{O}_2$	$\text{O}_2^{2-}$ or $\text{O}^-$	Lattice $\text{O}^{2-}$
<b><math>\text{LaFeO}_{3-\delta}</math></b>	25.55%	48.93%	18.69%	6.83%
<b><math>\text{LaFe}_{0.5}\text{Ni}_{0.5}\text{O}_{3-\delta}</math></b>	18.33%	29.47%	21.16%	31.05%
<b><math>\text{LaFe}_{0.5}\text{Ni}_{0.5}\text{O}_{3-\delta}/\text{N}</math></b>	15.43%	25.59%	28.80%	30.17%

Table S5. OER activities of perovskite oxides.

Catalysts	Overpotential@10 mA cm <sup>-2</sup> (mV)	Tafel (mV dec <sup>-1</sup> )	References
<b>LaFe<sub>0.5</sub>Ni<sub>0.5</sub>O<sub>3-δ</sub></b>	<b>281.4</b>	<b>75</b>	<b>This work</b>
<b>LaFe<sub>0.5</sub>Ni<sub>0.5</sub>O<sub>3-δ</sub>/N</b>	<b>270.6</b>	<b>65</b>	<b>This work</b>
<b>LaFe<sub>0.2</sub>Ni<sub>0.8</sub>O<sub>3</sub></b>	420	89	1
<b>3D microporous LaFe<sub>0.8</sub>Co<sub>0.2</sub>O<sub>3</sub></b>	410	56	2
<b>La<sub>0.5</sub>Sr<sub>0.5</sub>Ni<sub>0.4</sub>Fe<sub>0.6</sub>O<sub>3-δ</sub></b>	342	85	3
<b>SrNb<sub>0.1</sub>Co<sub>0.7</sub>Fe<sub>0.2</sub>O<sub>3-δ</sub></b>	370	48	4
<b>NdBaMn<sub>2</sub>O<sub>5.5</sub></b>	370	75	5
<b>LaNi<sub>0.8</sub>Fe<sub>0.2</sub>O<sub>3-δ</sub>-NR</b>	302	50	6
<b>PrBaCo<sub>2</sub>O<sub>5.75</sub></b>	360	70	7
<b>LaNi<sub>0.96</sub>Ir<sub>0.04</sub>O<sub>3</sub></b>	280	62	8
<b>LaCoO<sub>3</sub>/N-rGO</b>	560	65	9
<b>LaNiO<sub>3</sub>/NiO</b>	346	73	10
<b>BaCo<sub>0.4</sub>Fe<sub>0.4</sub>Zr<sub>0.1</sub>Y<sub>0.1</sub>O<sub>3-δ</sub></b>	324	69	11
<b>La<sub>2</sub>NiMnO<sub>6</sub></b>	370	58	12

## References

- [1] D. Zhang, Y. Song, Z. Du, L. Wang, Y. Li and J. B. Goodenough, *J. Mater. Chem. A*, 2015, **3**, 9421-9426.
- [2] J. Dai, Y. Zhu, Y. Zhong, J. Miao, B. Lin, W. Zhou and Z. Shao, *Adv. Mater. Interfaces*, 2018, **6**, 1801317.
- [3] C. C. Wang, Y. Cheng, E. Ianni, S. P. Jiang and B. Lin, *Electrochim. Acta*, 2017, **246**, 997-1003.



- [4] Y. Zhu, W. Zhou, Y. Zhong, Y. Bu, X. Chen, Q. Zhong, M. Liu and Z. Shao, *Adv. Energy Mater.*, 2016, **7**, 1602122.
- [5] C. Chen, Z. Wang, B. Zhang, L. Miao, J. Cai, L. Peng, Y. Huang, J. Jiang, Y. Huang, L. Zhang and J. Xie, *Energy Storage Mater.*, 2017, **8**, 161-168.
- [6] H. Wang, J. Wang, Y. Pi, Q. Shao, Y. Tan and X. Huang, *Angew. Chem. Int. Ed.*, 2019, **58**, 2316-2320.
- [7] X. Miao, L. Wu, Y. Lin, X. Yuan, J. Zhao, W. Yan, S. Zhou and L. Shi, *Chem. Commun.*, 2019, **55**, 1442-1445.
- [8] J. Li, L. Zheng, B. Huang, Y. Hu, L. An, Y. Yao, M. Lu, J. Jin, N. Zhang, P. Xi and C. H. Yan, *Small*, 2022, **18**, 2204723.
- [9] K. Liu, J. Li, Q. Wang, X. Wang, D. Qian, J. Jiang, J. Li and Z. Chen, *J. Alloys Compd.*, 2017, **725**, 260-269.
- [10] Y. Wei, Y. Zheng, Y. Hu, B. Huang, M. Sun, P. Da, P. Xi and C. H. Yan, *ACS Appl. Mater. Interfaces*, 2022, **14**, 25638-25647.
- [11] X. Li, J. Zhang, Q. Feng, C. Pu, L. Zhang, M. Hu, X. Zhou, X. Zhong, W. Yi, J. Tang, Z. Li, X. Zhao, H. Li and B. Xu, *J. Mater. Chem. A*, 2018, **6**, 17288-17296.
- [12] Y. Tong, J. Wu, P. Chen, H. Liu, W. Chu, C. Wu and Y. Xie, *J. Am. Chem. Soc.*, 2018, **140**, 11165-11169.